First principles study of various sodium-oxide molecules on N-doped graphene for high-performance $Na-O_2$ battery

C Fwalo [1, 2, *] and R E Mapasha[1,3]

[1]*Department of Physics, University of Pretoria, Hatfield, Pretoria, 0028, South Africa*

[2] Department of Physics, Copperbelt University, Riverside, Kitwe, 10101, Zambia

[3]*National Institute for Theoretical and Computational Sciences, Matieland, Private Bag X1, South Africa*

*Email:fwalochewe99@gmail.com

Abstract. To discover a material that can help mitigate issues surrounding the practical implementation of the sodium-oxygen battery (SOB), various materials, including 2D materials such as nitrogen-doped graphene (NGr), have been investigated due to their exceptional properties, like large surface area and excellent ion transport. However, there has been limited reporting on its use as a cathode additive in SOB. In this study, we investigated the adsorption mechanisms of various sodium oxides (Na_xO_2, where x = 1, 2, 3, and 4) on nitrogen-doped NGr, employing density functional theory (DFT). The results indicated that the discharge products are strongly anchored with binding energies ranging between -0.36 and -0.89 eV. These values suggest that NGr can effectively prevent the discharge products from easily dissociating into the electrolyte during electrochemical processes. Moreover, examining the complex charge density distributions supports the strong interactions between the molecules and the substrate. Notably, we observed that the metallic properties of the material were enhanced and preserved after adsorption, which is crucial for ion transport during battery operation. Overall, the findings suggest that NGr is a promising candidate for the next-generation SOB.

1. Introduction

Due to the increase in technological advancements, there has been a growing energy demand, leading to a higher reliance on fossil fuels, which significantly contributes to the effects of climate change. In light of this, scientists and engineers are making concerted efforts to develop energy-storing systems that can surpass the energy density of fossil fuels. While lithium-ion batteries (LIBs) possess high energy and power densities, they also face several limitations [1, 2]. Consequently, alternative systems such as metal-air batteries, including sodium- oxygen batteries (SOB) [1], are being considered for their exceptional properties, such as high theoretical capacity and low operational costs. However, SOB encounter challenges like weak adsorption of discharge products and poor conduction in the cathode during the discharging process, which hinder its practical implementation.

Given that the cathode is the component most affected by these issues, numerous materials have been investigated as potential cathode additives. Among these, graphene and nitrogen-doped graphene (NGr) are at the forefront of this investigation due to their remarkable properties, including large surface area, lightweight nature, excellent ion transport, and mechanical strength [2, 3, 4].

Despite extensive studies on NGr as a potential cathode for metal-air batteries [4], there remains a knowledge gap regarding the mechanisms of various sodium oxides (Na_xO_2) on NGr, which can leverage its excellent properties to revolutionize SOB technology. In this study, we employed density functional theory (DFT) to investigate the adsorption and diffusion mechanisms of various Na_xO_2 on NGr, aiming to determine their influence on the effectiveness of NGr as a cathode additive for the efficient sodium-oxygen battery (SOB). We systematically optimized the configurations, calculated the adsorption energies, and assessed their corresponding charge density distributions. Additionally, we calculated the bands structures to evaluate the stability of electronic conductivity post-adsorption.

2. Computational Methods

All the density functional theory (DFT) calculations were performed using Quantum ESPRESSO [5]. The generalized gradient approximation (GGA) [6] within the Perdew-Burke-Ernzerhof (PBE) functional [7] was employed to treat the exchange and correlation energies. To model the core electrons in the systems, we utilized the projector augmented wave (PAW) potential [8] as a pseudopotential. A kinetic energy cut-off of 544 eV was applied, using a plane-wave basis set to obtain the ground state energy. The Monkhorst-Pack scheme [9] was implemented with a K-points mesh of 6 x 6 x 1 within the Brillouin zone [10]. A nitrogen-doped graphene (NGr) supercell of size 4 x 4 x 1 (containing 32 carbon atoms) was modeled and subsequently optimized. The optimization involved fully relaxing the structure until all atomic positions converged within an energy difference of 10^{-5} eV, with a Hellman-Feynman force convergence criterion set to 10^{-6} eV/Å. The Methfessel-Paxton (MP) occupational function [11] was adopted for electron smearing. To minimize the influence of periodic images, a vacuum of 15 Å along the C-axis was included in the model.

The adsorption energies (E_{ads}) of various Na_xO_2 were determined using the following expression:

$$E_{ads} = \frac{E_{(complex)} - E_{(NGr)} - n * E_{(adsorbate)}}{n} \quad (1)$$

Where $E_{(complex)}$ is the total energy of the substrate adsorbed with the adsorbate, $E_{(NGr)}$ is the total energy of the pristine NGr, and $E_{adsorbate}$ is the total energy of the free-adsorbate.

For the charge density difference between the adsorbate and graphene, we adopted the following equation:

$$\Delta\rho = \rho_{(adsorbate+NGr)} - \rho_{(isolated-NGr)} - \rho_{(adsorbate)}. \quad (2)$$

Here, $\rho_{(adsorbate+NGr)}$ is the charge of the substrate with the adsorbate, $\rho_{(isolated-adsorbate)}$ is the charge of the adsorbate detached from the complex, and $\rho_{(isolated-NGr)}$ is the charge of the substrate detached from the complex.

3. Results and Discussions

3. 1. Optimized configurations and Charge density distributions of NaO_2 *and* Na_4O_2 *on NGr*

The operation of a battery follows a processes of discharge and charging, where during the discharging process the oxidized anode produces the Na ion which diffuse via the electrolyte towards the cathode and reacts with the oxygen which diffuses the system through the porous cathode to form various Na_xO_2 along the process as shown in Equation 3. And during the reverse, which is the charging process, the formed Na_xO_2 breaks down, with Na-ions diffusing back to the anode and O_2 diffusing outside the ambient environment. Notably, from the discharge products, NaO_2 and Na_4O_2 are considered to be the most stable and least stable, respectively. Hence, they are being intensively investigated for a comprehensive understanding of the battery operations. The following mechanisms depicts what takes place during the electrochemical processes in the battery:

$$NGr + Na^+ + e^- + O_2 \rightarrow \underline{NaO_2@NGr} \quad (3)$$

$$NaO_2@NGr + Na^+ + e^- \rightarrow \underline{Na_2O_2@NGr}$$

$$Na_2O_2@NGr + Na^+ + e^- \rightarrow Na_3O_2@NGr$$

$$Na_3O_2@NGr + Na^+ + e^- \rightarrow Na_4O_2@NGr.$$

The adsorption energy of the electrode material is very important to ascertain its ability to enhance the performance of the battery. To accurately calculate this significant property, the molecule and isolated NGr substrate were fully optimized separately as shown in Figure 1. Consequently, the configurations of the molecules on NGr were fully optimized as shown in Figure 2b, followed by the calculation of their corresponding adsorption energies. Therefore, we calculated the adsorption energies of all species taking part in the overall electrochemical processes, and the results are presented in Table 1.

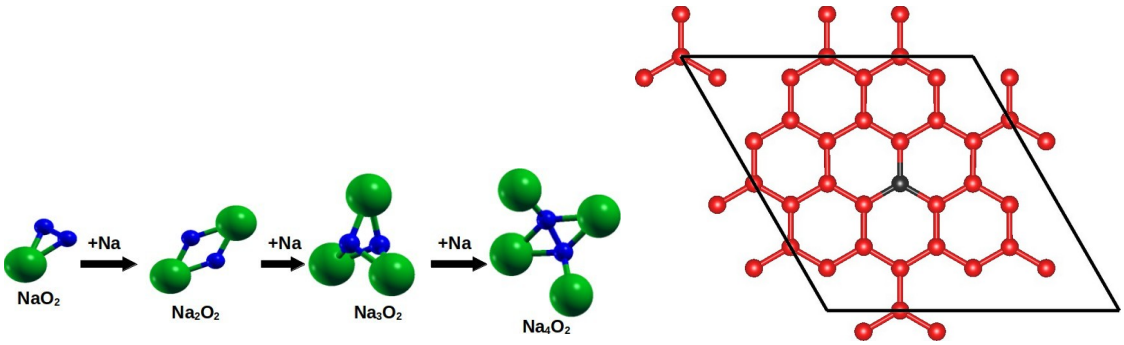

(a) (b)

Figure 1: Optimized molecules of various Na_xO_2, and NGr supercell of size 4 x 4 x 1, consisting of 32 carbon atoms.The green, black, red and blue balls denote sodium (Na), nitrogen (N), carbon (red) and oxygen(O) atoms, respectively.

The results revealed that all the discharge products are strongly anchored with values ranging from -0.36 to -0.89 eV, strong enough to prevent them from dissociation into the electrolyte during the discharging process. This is significant as it helps to enhance the cycle life of the battery.

Table 1: Calculated E_{ads} (eV), and charge density (|e|) of various Na_xO_2 on NGr

System	**Eads (eV)**	**Charge density |e|**
NaO_2	-0.36	0.04
Na_2O_2	-0.62	0.45
Na_3O_2	-0.54	0.95
Na_4O_2	-0.89	1.00

As the adsorption takes place on the surface of the NGr, the species are observed to have been strongly attached. This shows the interaction been the NGr and the adsorbate. Therefore, to check the extent of the interaction, the microscopic mechanisms of the electron being shared in the system are very significant to be known. To accomplish this, we calculated the charge density distribution in the systems of NaO_2 and Na_4O_2 as illustrated in Figures 2a and 2b, repectively. Additionally, the quantity of the charge densities was calculated as detailed in Table 1, and It was found that the charge was transfered from Na_xO_2 and NGr, with accumulation (yellow) from the Na ions towards the surface of NGr for all the systems investigated (Figure 2). Notably, charge depletion was observed between the oxygen atoms, suggesting its high affinity for electrons.

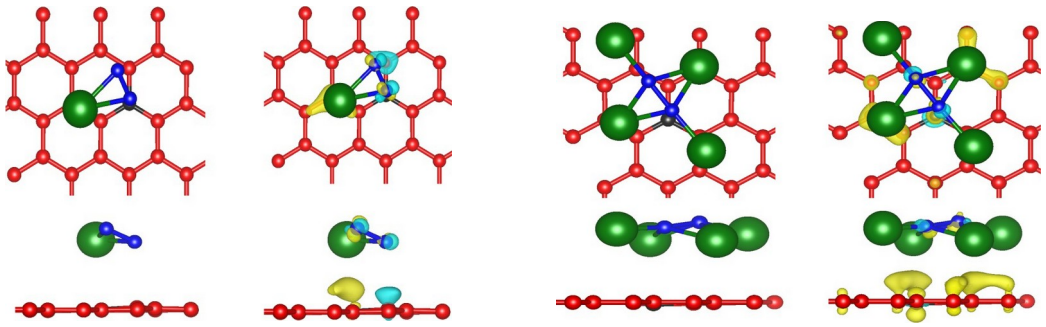

(a) (b)

Figure 2: Optimized Configurations and Charge density distributions of NaO_2 and Na_4O_2 on the NGr :(a) NaO_2, (b) Na_4O2. Where charge accumulation and depletion are denoted by the colors yellow and cyan, respectively.

Ultimately, the charge distributions and quantity being transferred show evidence of electronic interaction of the discharge products with the NGr. This is very important for optimal battery operation.

3. 2. Metallic characteristics of NGr adsorbed with various Na_xO_2

The electronic conductivity of any material as an electrode is very significant the enhanced battery operation. Therefore, before being used as an electrode, the metallic properties are investigated. In this work, we investigated the pristine graphene (Gr), NGr, and post-adsorption of the NaO_2 and

Na_4O_2. The results showed that Gr is semi-metallic with cone Dirac along the Fermi level as shown in Figure 3a. The obtained results are similar to the previous reported study [4].

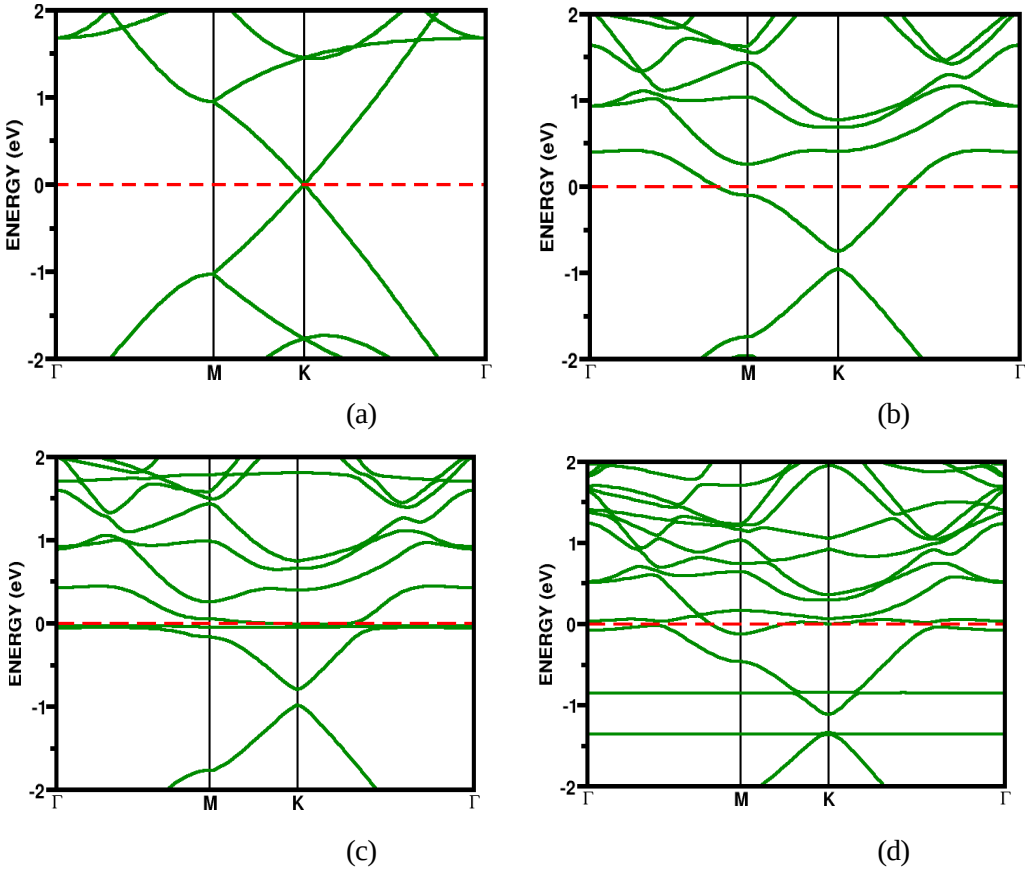

Figure 3: **Bands structure of NGr adsorbed with** Na_xO_2 **:** (a) pristine G, (b) pristine NG, (c), NaO_2, and (c) Na_4O_2. The dashed red line denotes the Fermi level.

For the NGr, it was found that the metallic properties are enhanced as shown in Figure 3b, this is very significant for battery operations, as it shows the capability of the material to be able to charge and discharge the ions during the operation. Hence, improving the cycle life of the system. After the adsorption of Li_2S (Figure 3c), the Fermi level was observed to have shifted upwards as the bands moved towards, showing the enhanced electronic conduction in the system. This trend was similarly observed for the system of Na_4O_2 (Figure 3d), where the Fermi level moved upwards and bands downwards. Suggesting that not only were the metallic properties preserved, but also enhanced. Overall, the adsorption of the non-conductive various Na_xO_2 on NGr improves its electronic conductivity, which is very important for the optimal operation of the battery.

4. Conclusion

In summary, DFT was to explore the adsorption and diffusion mechanisms of Na_xO_2 on NGr and assess their impact on its electronic properties. The findings indicated that Na_xO_2 species are strongly adsorbed on NGr, highlighting its essential role in preventing dissociation into the electrolyte during the discharging process. Moreover, the calculated charge density distributions

revealed significant electronic interactions between the discharge products and NGr, with charge sharing evident from the iso-surfaces. Notably, the metallic characteristics of NGr were preserved despite the adsorption of non-conductive Na_xO_2, suggesting that NGr effectively mitigates poor conductivity and premature dissociation issues. This supports the potential for developing a practically implemented SOB.

Conflicts of interests

The authors declare no conflict of interest.

Acknowledgements

The University of Pretoria, through the Department of Innovation and Research, is acknowledged for supporting this project financially. Additionally, the Center for High-Performance Computing (CHPC) in Cape Town, South Africa, is acknowledged for providing us with computational resources (Project name: MATS1429). R.E.M. recognises the National Institute for Theoretical and Computational Sciences (NTheCS) for the financial support.

References

[1] J. W. Choi, D. Aurbach, Promise and reality of post-lithium-ion batteries with high energy densities, Nature reviews materials 1 (4) (2016) 1–16.
[2] C. Xia, C. Kwok, L. Nazar, A high-energy-density lithium-oxygen battery based on a reversible four-electron conversion to lithium oxide, Science 361 (6404) (2018) 777–781.
[3] S. K. Das, S. Lau, L. A. Archer, Sodium–oxygen batteries: a new class of metal–air batteries, Journal of Materials Chemistry A 2 (32) (2014) 12623–12629.
[4] P. Avouris, C. Dimitrakopoulos, Graphene: synthesis and applications, Materials Today 15 (3) (2012) 86–97.
[5] J. H. Lee, S. G. Kang, I. T. Kim, S. Kwon, I. Lee, S. G. Lee, Adsorption mechanisms of lithium oxides (lixo2) on n-doped graphene: a density functional theory study with implications for lithium–air batteries, Theoretical Chemistry Accounts 135 (3) (2016) 50.
[6] P. Giannozzi, O. Andreussi, T. Brumme, O. Bunau, M. B. Nardelli, M. Calandra, R. Car, C. Cavazzoni, D. Ceresoli, M. Cococcioni, et al., Advanced capabilities for materials modelling with quantum espresso, Journal of Physics: Condensed Matter 29 (46) (2017) 465901.
[7] S. Grimme, Semiempirical GGA-type density functional constructed with a long-range dispersion correction, Journal of Computa- tional Chemistry 27 (15) (2006) 1787–1799.
[8] J. P. Perdew, K. Burke, M. Ernzerhof, Perdew, burke, and ernzerhof reply, Physical Review Letters 80 (4) (1998) 891.
[9] P. E. Blöchl, Projector augmented-wave method, Physical review B 50 (24) (1994) 17953.
[10] H. J. Monkhorst, J. D. Pack, Special points for brillouin-zone integrations, Physical Review B 13 (12) (1976) 5188.
[11] D. J. Chadi, Special points for brillouin-zone integrations, Physical Review B 16 (4) (1977) 1746.
[12] M. Methfessel, A. Paxton, High-precision sampling for brillouin-zone integration in metals, physical review B 40 (6) (1989) 3616.